LUND UNIVERSITY

Multi-colour fluorescence imaging in connection with photodynamic therapy of delta-amino levulinic acid (ALA) sensitised skin malignancies

Andersson-Engels, Stefan; Berg, R; Svanberg, Katarina; Svanberg, Sune

Published in:
Bioimaging

DOI:
10.1002/1361-6374(199509)3:3<134::AID-BIO4>3.0.CO;2-1

1995

Link to publication

Citation for published version (APA):
Andersson-Engels, S., Berg, R., Svanberg, K., & Svanberg, S. (1995). Multi-colour fluorescence imaging in connection with photodynamic therapy of delta-amino levulinic acid (ALA) sensitised skin malignancies. *Bioimaging*, *3*(3), 134-143. https://doi.org/10.1002/1361-6374(199509)3:3<134::AID-BIO4>3.0.CO;2-1

Total number of authors:
4

General rights
Unless other specific re-use rights are stated the following general rights apply:
Copyright and moral rights for the publications made accessible in the public portal are retained by the authors and/or other copyright owners and it is a condition of accessing publications that users recognise and abide by the legal requirements associated with these rights.
• Users may download and print one copy of any publication from the public portal for the purpose of private study or research.
• You may not further distribute the material or use it for any profit-making activity or commercial gain
• You may freely distribute the URL identifying the publication in the public portal

Read more about Creative commons licenses: https://creativecommons.org/licenses/

Take down policy
If you believe that this document breaches copyright please contact us providing details, and we will remove access to the work immediately and investigate your claim.

LUND UNIVERSITY

PO Box 117
221 00 Lund
+46 46-222 00 00

Bioimaging **3** (1995) 134–143. Printed in the UK

Multi-colour fluorescence imaging in connection with photodynamic therapy of δ-amino levulinic acid (ALA) sensitised skin malignancies

Stefan Andersson-Engels†‡‖, Roger Berg†‡, Katarina Svanberg†§ and Sune Svanberg†‡

† Lund University Medical Laser Centre, Lund Institute of Technology, PO Box 118, S-221 00 Lund, Sweden
‡ Department of Physics, Lund Institute of Technology, PO Box 118, S-221 00 Lund, Sweden
§ Department of Oncology, Lund University Hospital, S-221 85 Lund, Sweden

Submitted 23 January 1995, accepted 2 November 1995

Abstract. A system for multi-colour fluorescence imaging of tissue is described. The instrument is mainly developed for tissue diagnostics to identify and localise malignant tumours, but might also be useful for real-time monitoring of the therapeutic dose delivered during photodynamic therapy. *In vivo* examples from various malignant skin lesions following topical δ-amino levulinic acid (ALA) administration are presented. The diagnostic system utilises both characteristics of a fluorescent tumour marker, such as a porphyrin containing substance, and the native tissue autofluorescence to characterise the tissue. A dimensionless function of three or four simultaneously recorded fluorescence intensities is formed and an optimum-contrast image is calculated pixel-by-pixel.

Keywords: tissue diagnostics, fluorescence spectroscopy, imaging, skin cancer, photosensitiser, ALA.

1. Introduction

Photodynamic therapy (PDT) is gaining interest in the local treatment of certain types of malignancies, although the approval process for the first generation photosensitiser—Photofrin—seems to be very slow. The long evaluation time has mainly been due to the conceptually new treatment modality and the poorly characterised chemical substance used. In parallel with the clinical evaluation of Photofrin, it is now of interest to develop and evaluate second-generation photosensitisers for PDT. Phase I–II clinical trials have been initiated for several substances such as benzoporphyrin derivative, zink-phthalocyanin and *meso*-tetrahydroxy phenyl chlorin and phase III trials for δ-amino levulinic acid (ALA). ALA, a precursor in the haem cycle, is itself not a photosensitiser, but in excess quantities it will cause photodynamic active protoporphyrin to accumulate in tissue. Protoporphyrin is an intermediate product in this cycle, and is the origin both for the characteristic dual-peaked porphyrin fluorescence at 635 and about 700 nm and photosensitisation of living tissue following ALA administration. ALA has been shown to be especially useful after topical application, reducing the only side-effect with PDT described to date in the literature—skin photosensitisation following intravenous injection of Photofrin. ALA-PDT was first applied to humans by Kennedy *et al* (1990) and has been successfully used for PDT of skin malignancies (Kennedy *et al* 1992, Svanberg *et al* 1994).

Diagnostic techniques using porphyrin fluorescence as a tumour marker have been developed. These techniques have been developed in parallel with photodynamic therapy utilising porphyrin photosensitisation of various types of malignancies (Profio 1990, Andersson-Engels and Wilson 1992). The interest so far has mostly been to develop various kinds of instrumentation for early tumour

‖ e-mail: Stefan.Andersson-Engels@fysik.lth.se

0966-9051/95/030134+10$19.50 © 1995 IOP Publishing Ltd

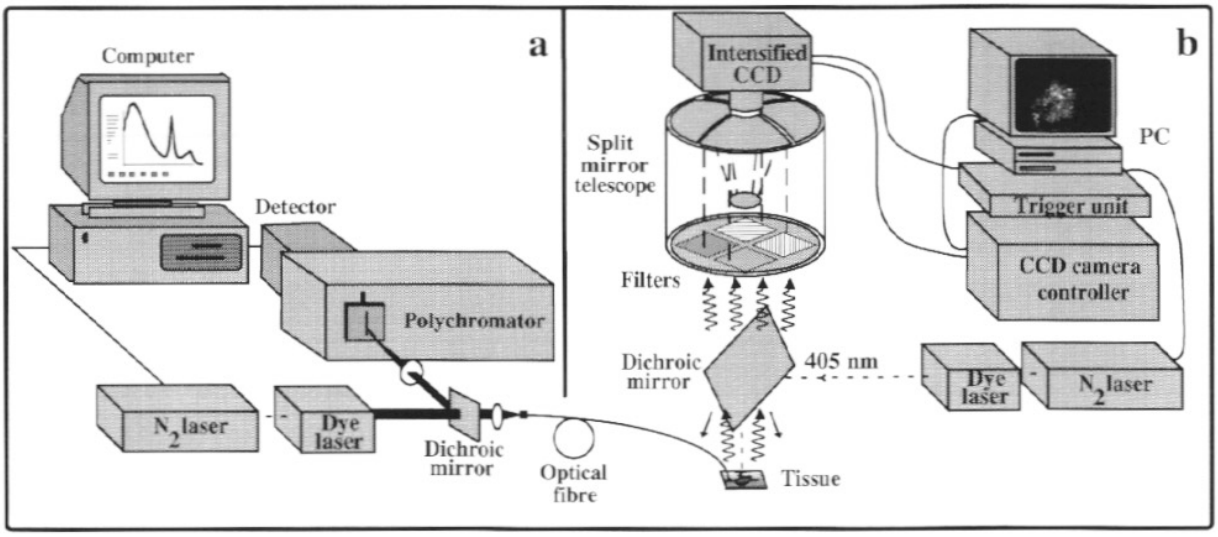

Figure 1. Arrangements for (a) the spectrally resolving point-measuring fluorosensor and (b) the multi-colour fluorescence imaging system.

Table 1. Patient data and results from the fluorescence imaging system. A central area over the tumour represents the tumour values and an area between 3 and 5 mm outside the visible tumour border is used for the skin values. The ratio of the processed values for the tumour and skin areas are given together with the tumour identification quality Q, defined in (2) as a ratio of the difference between the tumour and skin function values, and the square root of the sum of their variances. This quality Q gives a measure of how much the function value increases going from the skin to the tumour in comparison with the variation of these values within the two areas. Nod: Nodular; Sup: Superficial; BCC: basal cell carcinoma; Cut: Cutaneous; Mb. Bowen: squamous cell carcinoma *in situ*.

	Patient data			Malignant tumour			Imaging results	
No	Initials	Sex	Age	Type	Size (mm) length × width	Location	Ratio tum/skin	Q
1	G.B.	F	63	Nod. BCC	20 × 20	scalp	25	2.6
2	A.S.	F	73	Nod. BCC	9 × 8	nose	6.2	2.4
3	J.P.	M	36	Nod. BCC	9 × 7	eyelid	3.8	1.4
4	L.S.	M	48	Nod. BCC	15 × 15	chin	5.2	1.2
5	T.B.	M	77	Nod. BCC	30 × 20	forehead	20	2.6
				Sup. BCC	20 × 18	back	18	2.4
6	D.J.	F	85	Mb. Bowen	60 × 58	lower leg	22	2.3
7	M.A.	F	88	Cut. T-cell lymphoma	70 × 60	upper arm	58	5.3

detection. Less attention has been paid to an evaluation of instrumentation and detection limits for various tumour types. This is mainly due to the present restrictions on the photosensitiser used as a fluorescent tumour marker, hampering clinical studies. Another, much less exploited area for fluorescence probing instruments, is to measure the photo-bleaching of the photosensitiser during PDT and use this parameter as an on-line input for PDT dosimetry (Andersson *et al* 1992). Porphyrin photobleaching has been the subject of several studies (Moan 1988, Moan *et al* 1988, Schneckenburger *et al* 1989). None has, however, considered measuring the photobleaching and using this signal as a dosimeter parameter. Several groups have developed detection criteria for tissue diagnosis making use also of the native tissue autofluorescence (Andersson-Engels *et al* 1991, Lam *et al* 1993, Lohmann *et al* 1989). In this way it is possible to find a more robust diagnostic criterion as well as more information about the tissue under study. Firstly, one would like to be able to subtract the superimposed tissue autofluorescence from the tumour marking agent fluorescence to gain contrast. Secondly, one would like to divide the background-free fluorescence

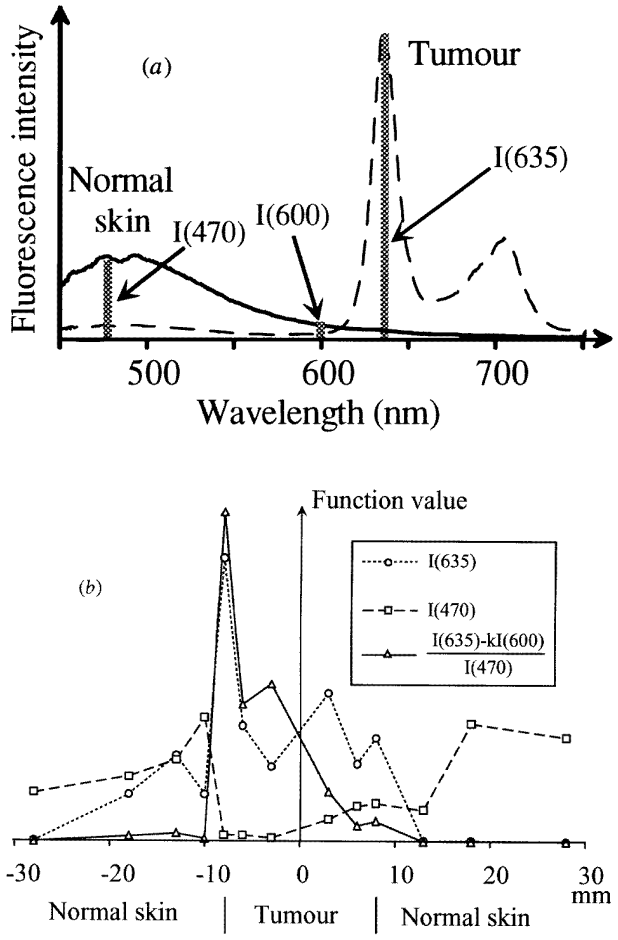

Figure 2. (a) Typical fluorescence emission spectra from an ALA-sensitised tumour and surrounding normal skin. The two strong peaks at 635 nm and 700 nm from the tumour area result from the protoporphyrin produced in the tissue due to the presence of an excess amount of ALA. The broad tissue autofluorescence around 500 nm is lower in the tumour area than in the surrounding skin. The wavelengths used in the imaging system are indicated. The excitation wavelength was 405 nm. (b) A fluorescence scan from normal skin, across a tumour and out on normal skin on the other side of the tumour, as obtained by evaluating the fluorescence intensities at indicated wavelengths from the fluorescence spectra recorded with the point monitoring system.

from the tumour marker by the tissue autofluorescence, as this is known to often be lower in the tumour than in the surrounding normal tissue, further enhancing the tumour detection capabilities. In this way the full spectroscopic information from the tissue autofluorescence can be included in the diagnostic criterion. At the same time, by forming a ratio of fluorescence intensities, the influences of variations in excitation energy and detection geometry can be reduced. Diagnostic instrumentation developed for the detection of small early tumours or the extent of a known tumour should produce images of the tissue. Recently, several fluorescence imaging systems for tissue diagnostics have been described (some of them by Andersson *et al* 1987, Hirano *et al* 1989, Unsöld *et al* 1990, Palcic *et al* 1991). To investigate the potential of such a system for medical diagnostics, an experimental system was constructed in our laboratory (Andersson-Engels *et al* 1994). In that paper an investigation of the system performance, with the aim of being able to optimise the design of possible future clinically adapted multi-colour fluorescence imaging systems, is presented. These considerations were taken into account in assembling the imaging system used in this study. In the present paper the first clinically obtained images from the system developed in our group are presented. Examples from basal cell carcinoma lesions, an *in situ* squamous cell carcinoma lesion and a cutaneous T-cell lymphoma, topically given ALA in a cream for 4–6 hours, are presented. These lesions were chosen because they are easily accessible to us within a running program for PDT. Furthermore, although they usually are easy to diagnose and have marked borders for a naked eye examination, the lesions seldom do not exhibit a wider spread than these visible borders. This spread could be detected with a fluorescence examination.

2. Material and methods

2.1. Instrumentation

Tissue fluorescence spectra were obtained using a fluorosensor developed for clinical use. The system is described in detail by Andersson-Engels *et al* (1991), and is schematically illustrated in figure 1(a). Briefly, the system is based on optical fibre light guiding. This enables fluorescence recordings from the most advanced examinations or surgical procedures, as the contact with the patient is limited to a sterilised clear cut optical fibre tip. As an excitation source a small sealed-off nitrogen laser pumping a dye laser emitting at the protoporphyrin excitation peak at 405 nm was used. The laser system gave 3 ns long pulses. The pulses were passed through a small beam expander, reflected by a dichroic mirror and focused into an almost fluorescence free, 600 μm core diameter quartz fibre. The distal end of the fibre was placed in contact with the tissue to be examined. The energy of the laser pulses exiting the optical fibre was measured to be 10 μJ. The light was partly absorbed by molecules within the tissue and a fraction of the absorbed light gave rise to fluorescence. By using the same optical fibre for guiding the fluorescence back to the detector a reproducible measurement geometry was established. This detection geometry also allowed an efficient collection of the fluorescence as the excitation light only penetrates about 0.5 mm in tissue. The fluorescence was transmitted through the dichroic mirror and focused onto the entrance slit of a 27 cm polychromator. A polychromator with a 150 lines/mm grating and a focal ratio of F/3.8, matching the focused light from the optical fibre, was used. A cut-off

filter was placed in front of the entrance slit to suppress any stray light from the laser. The wavelength-dispersed light at the exit of the polychromator was detected using an image intensified diode array and stored and analysed in a multi-channel analyser. The tissue fluorescence spectra presented here are results of accumulations from 100 sequential laser pulses at a repetition rate of 15 Hz. The wavelength scale was calibrated using the mercury lines in a fluorescent tube light source. Variations in sensitivity with the wavelength for the entire detection system were corrected for by recording the output from a calibrated blackbody radiator and using this spectrum to produce a correction curve. All fluorescence spectra were multiplied with this correction curve.

The principles for our multi-colour fluorescence imaging system are given by Andersson *et al* (1987) and Andersson-Engels *et al* (1994). The optical arrangement of the presently used system is shown in figure 1(b). As an excitation source a sealed-off nitrogen laser (Laser Science Model 337ND) pumping a dye laser was used. Pulsed light at 405 nm at 20 Hz and with a pulse length of 3 ns resulted. This light was focused into a quartz optical fibre. The light was guided to uniformly irradiate a masked tissue area of about 25 mm $\times$ 35 mm. The tissue was placed in the object plane of a specially designed Cassegrainian telescope. The first mirror in the telescope was split into four segments, allowing four identical images to be produced of the object. By tilting each segment separately to produce the images just off the optical axis, one image in each of the four quadrants of an image intensified CCD camera (Spectroscopy Instruments ICCD) could be obtained. The image intensified detector allowed gated detection (a 100 ns gate width was used), and thus CW background-light could be efficiently suppressed. Separate optical filtration of the light for the four images yielded images of the tissue in four fluorescence passbands. The filters were centred on 470 nm (tissue autofluorescence peak), 600 nm (tissue autofluorescence close to the 635 nm porphyrin peak), 635 nm (porphyrin peak) and 670 nm (photobleaching signal), respectively. The filter bandwidths were 10–15 nm full width half maximum (FWHM). The images presented here are results of 5–30 seconds of light integration on the CCD chip. The camera was cooled to -30 degrees Celsius to decrease dark current build-up in the detector and a dark image was subtracted from each recording before further data processing. The data were digitised in a computer for processing and storage. Both the raw data and the processed images could be printed out using a colour laser printer.

2.2. Patients

Seven patients, five with basal cell carcinoma lesions, one with an *in situ* squamous cell carcinoma lesion and one with a cutaneous T-cell lymphoma, were investigated with the fluorescence imaging system in connection with photodynamic therapy. The tumour data are listed in table 1. All tumours were biopsy proven and photographic documentation was taken. The lesion size varied in the range of 8–60 mm in diameter. Powder of δ-amino levulinic acid (ALA) was dissolved in sterile water. An oil-in-water based cream with 20% by weight ALA was then prepared immediately before the topical application. The cream was applied on the tumours with a margin of about 15 mm and covered with an occlusion pad for 4–6 hours.

2.3. Animal

A Wistar/Furth rat was used to assess the possibilities of using the multi-colour imaging system for bleaching dosimetry. The liver was chosen for this bleaching experiment due to its homogenous structure and the even distribution of the photosensitiser. An ALA dose of 60 mg/kg body weight was injected into the femoral vein 1 hour *prior* to the photodynamic procedure. Following general anaesthesia using chloral hydrate, the abdomen was cut open and the right liver lobe was exposed. A mask of black paper was placed on the liver surface and an unmasked region was irradiated with 635 nm laser light. A total energy density of 15 J/cm^2 was delivered to the tissue at a light fluence rate of 70 mW/cm^2. Immediately following the irradiation both the masked and unmasked regions were imaged using the multi-colour fluorescence imaging system.

3. Results and discussion

The concept of the system is to measure four fluorescence intensities at different wavelengths for each spatial location of an image and to form an arithmetical function of these intensities giving optimal tumour contrast. The exact procedure is best understood by studying the shape of the fluorescence spectra from an ALA treated tumour and surrounding skin. Two main differences can be seen in figure 2(a). Firstly, the strongly dominating porphyrin peaks at 635 and 700 nm in the tumour spectrum are almost absent in the skin spectrum. Secondly, the tissue autofluorescence peaking at 470 nm is weaker in the tumour spectrum as compared with the normal skin. The evaluated fluorescence intensities at 635 nm (at the strong porphyrin peak), at 470 nm (corresponding to the tissue autofluorescence peak) and at 600 nm (the wavelength used to subtract the superimposed tissue autofluorescence from the porphyrin fluorescence at 635 nm) are indicated in figure 2(a). In figure 2(b) these fluorescence intensities are shown in a scan starting in normal skin, passing over a nodular basal cell carcinoma lesion and continuing in the normal skin at the opposite side. By forming the dimensionless function

$$F = \{I(635\ \text{nm}) - k \times I(600\ \text{nm})\}/I(470\ \text{nm}) \qquad (1)$$

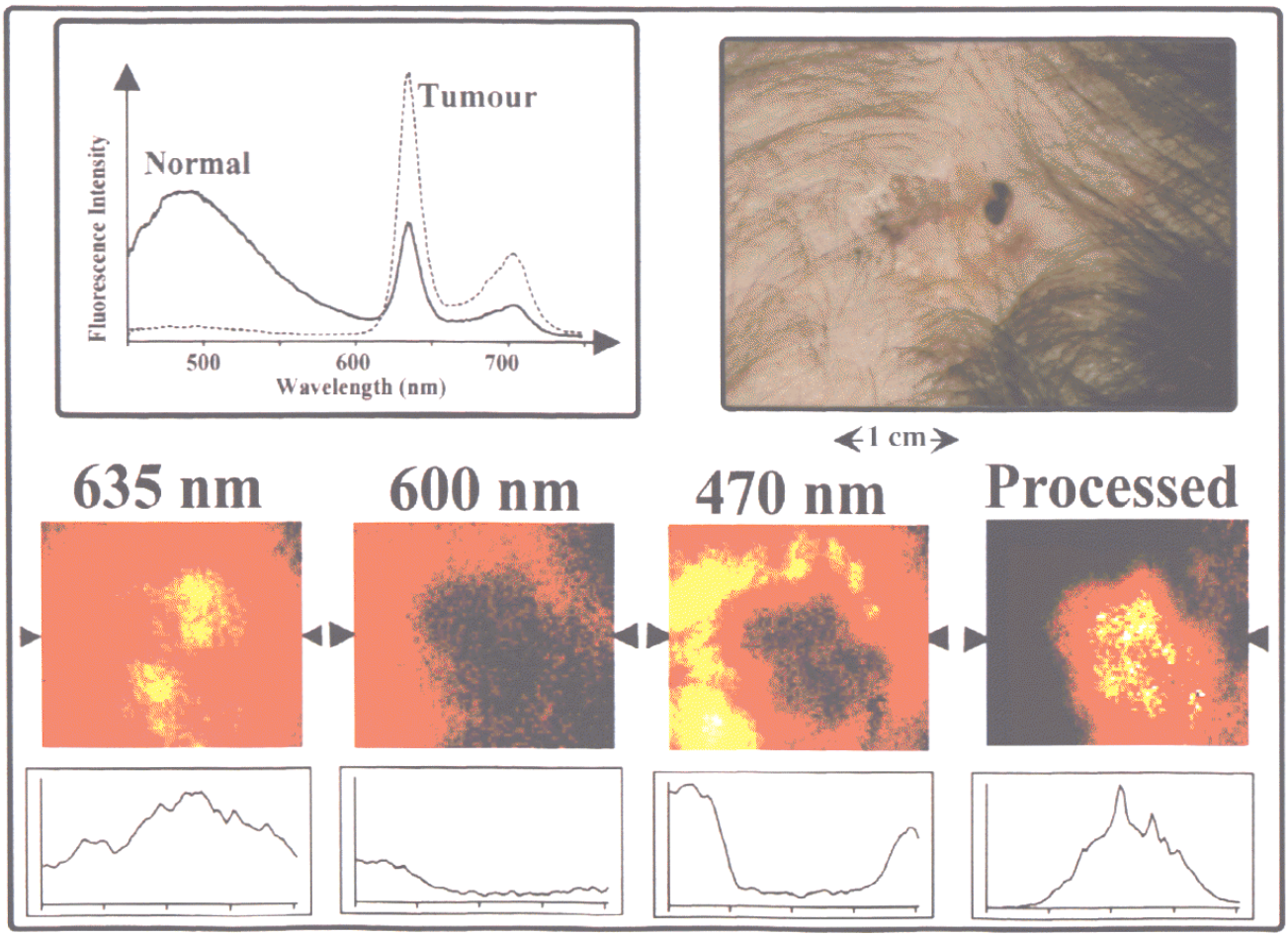

Figure 3. Fluorescence spectra of a nodular basal cell carcinoma lesion and surrounding normal skin on the skull, (photograph in the upper right corner), are presented at the upper left corner (Patient 1). Raw data fluorescence images from the central part of the photo at the three emission wavelengths utilised are shown below, together with the processed image using the function $F = \{I(635\text{ nm}) - k \times I(600\text{ nm})\}/I(470\text{ nm})$. False-colour coding was used in the presentation of the fluorescence images. Intensity data along a line between indicated locations through the images are also given. The excitation wavelength was 405 nm.

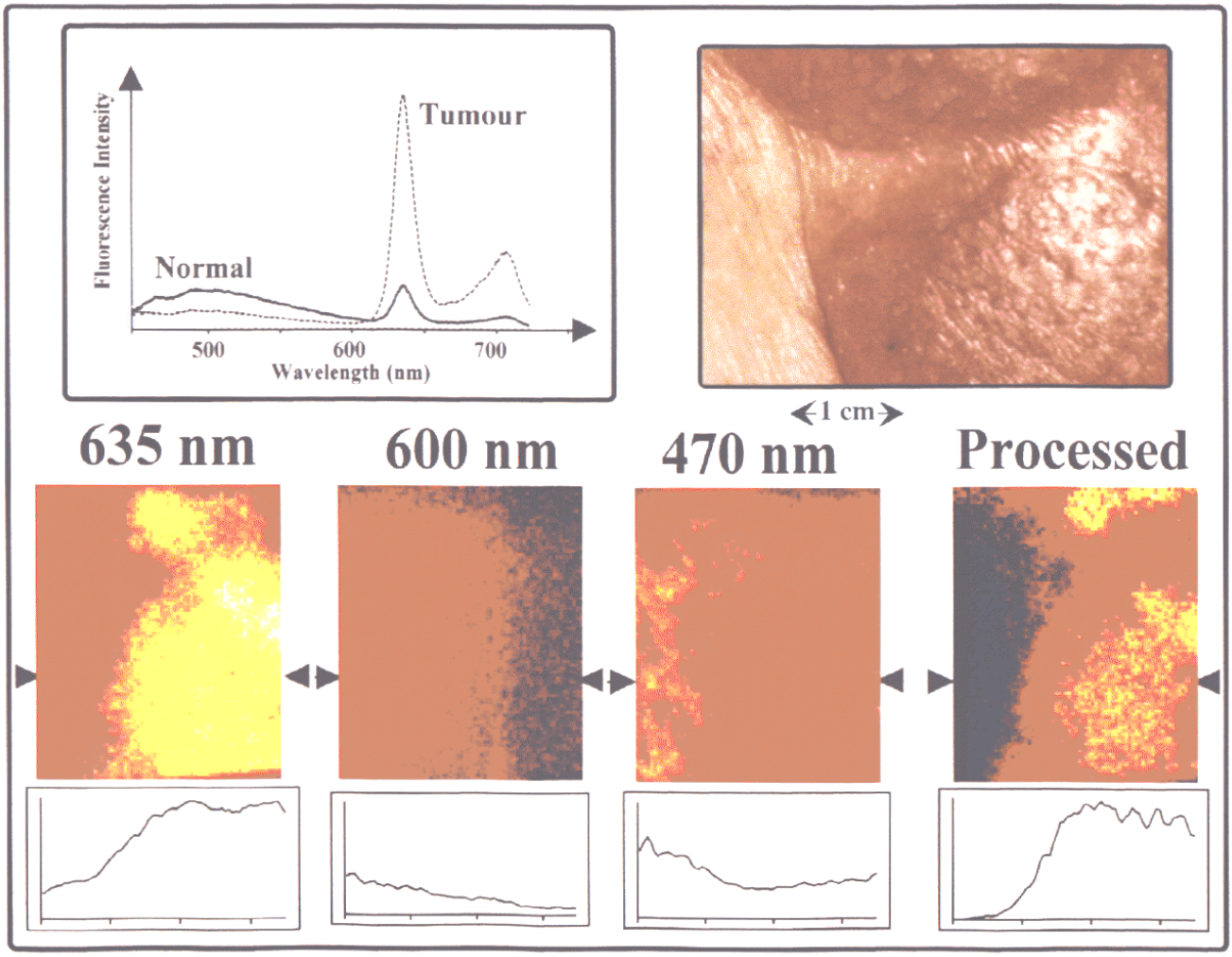

Figure 4. Fluorescence spectra and images as in figure 3 for a cutaneous T-cell lymphoma on the upper arm (Patient 7).

a good demarcation of the lesion is reached. The constant k is used to scale the tissue autofluorescence signal at 600 nm to have the same intensity as the autofluorescence superimposing the porphyrin signal at 635 nm. With the correct choice of the k-factor the true porphyrin signal at 635 nm is thus given by the numerator in (1). The value of k is typically 0.85. This means that the expression in (1) gives the pure porphyrin signal at 635 nm divided with the autofluorescence signal at 470 nm. This is exactly what the multi-colour imaging system achieves, but now in parallel in two dimensions.

The various steps in the formation of such a processed multi-colour fluorescence image are presented in figure 3 for a nodular basalioma lesion on the skull (Patient 1). Fluorescence spectra of the central region of the lesion as well as from the normal skin surrounding the lesion are shown in the figure. The three fluorescence images at 635 nm, 600 nm and 470 nm are presented together with intensity data along a line across the lesion between the indicated locations. Finally, the function image $F = \{I(635\text{ nm}) - k \times I(600\text{ nm})\}/I(470\text{ nm})$ is given with the F value displayed along the chosen line. The k value was set in such a way that the numerator was equal to zero for a normal skin region where no ALA had been applied. As can be seen, the function image yields the sharpest contrast of the lesion. The drastic decrease of the tissue autofluorescence in the tumour region strongly contributes to the demarcation of the tumour in the function image. The porphyrin signal extends outside the lesion border as judged by visual inspection, and gives only a minor tumour delineation in this case. No biopsy was taken from the seemingly normal skin surrounding the lesion, and thus it is impossible to judge whether this area was infiltrated by the tumour or not. A tumour and surrounding skin were treated with PDT immediately following the multi-colour imaging examination and a complete response at a following-up time of 10 months was achieved. The necrotic region one week after PDT was limited to the area delineated by the multi-colour fluorescence imaging system, suggesting that the tumour did not to a large extent infiltrate the surrounding tissue.

A similar arrangement of fluorescence information for a cutaneous T-cell lymphoma, using the three sub-images at 635 nm, 600 nm and 470 nm together with the processed function image, is presented in figure 4 (Patient 7). These images indicate a high porphyrin signal in the tumour and a less marked contrast in the tissue autofluorescence. Also in this case, with three raw-data images looking quite differently from those in figure 3 (it is another tumour type), the processed image gives a sharp demarcation of the lesion. In this case good delineation of the tumour is due to a contrast in both the porphyrin and the tissue autofluorescence signals.

Diagnostic data about all the patients included in this study are indicated in table 1. It further presents the ratio of the average F-function value of a central tumour area and an area between 3 and 5 mm outside the gross tumour border. Far outside the tumour area no porphyrin could be detected and thus the function value goes to zero. Close to the border the multi-colour fluorescence imaging system marked the various tumours differently. Except for patients 2, 3 and 4, the ratio of the function values for the tumour centre and a region 3–5 mm outside the grossly seen tumour border, was high, indicating a sharp demarcation of the tumours. We also calculated the tumour identification quality Q for the system as the ratio between the difference between the mean values for the tumour and skin areas, and the square root of the sum of their variances

$$Q = \frac{\bar{F}_{\mathrm{T}} - \bar{F}_{\mathrm{S}}}{(\sigma_{\mathrm{T}}^2 + \sigma_{\mathrm{S}}^2)^{1/2}} \tag{2}$$

where $\bar{F}_{\mathrm{T}}$ and $\bar{F}_{\mathrm{S}}$ are the average function value for the tumour and skin regions, respectively, and σ_{T} and σ_{S} are the corresponding standard deviations. This quality function showed a good demarcation for all tumours, except for patients 3 and 4. A tumour spread outside the obviously visible tumour borders could be suspected for these tumours. No biopsies were, however, taken from the measured regions, and thus the tumour border is not fully known. In other studies the potential of fluorescence techniques to identify early malignant lesions and to delineate the tumour borders of identified tumours have been investigated in more detail and compared with extensive biopsy sampling. In a pure spectroscopic study using the point-measuring system, shown in figure 1(a), it was shown that tumours spread outside the visible borders could be detected using fluorescence. Other studies indicate that benign naevi have a fluorescence signal different from those of malignant lesions (Lohmann and Paul 1989, Svanberg *et al* 1995).

Figure 5 shows the shape of the fluorescence spectra of a basal cell carcinoma lesion *pre* and *post* PDT. As can be seen, the porphyrin signals have effectively been bleached due to the laser treatment, while the blue–green tissue autofluorescence remains unaltered. A dose of about 20 J/cm^2 caused the 635 nm peak to bleach to $1/e$ of its original value. Also, the spectral shape in the red spectral region had changed after the laser irradiation. After PDT a shoulder at about 670 nm had developed in the fluorescence spectrum. This shoulder originates from photodegradation products of the sensitiser caused by the light (Moan *et al* 1988, König *et al* 1990). By relating the intensity of this shoulder to the sensitiser signal at 635 nm, a number dependent on the absorbed light dose can be extracted (Andersson *et al* 1992). Andersson *et al* showed that the dimensionless $I(670\text{ nm})/I(635\text{ nm})$ ratio was 0.15 for an untreated basalioma and 0.30 after a light dose of 40 J/cm^2. In figure 6 an image of a rat liver surface, including both an irradiated and a non-irradiated area, is presented in this function, $F = I(670\text{ nm})/I(635\text{ nm})$. As can be seen in this processed image, the region irradiated by 15 J/cm^2 was

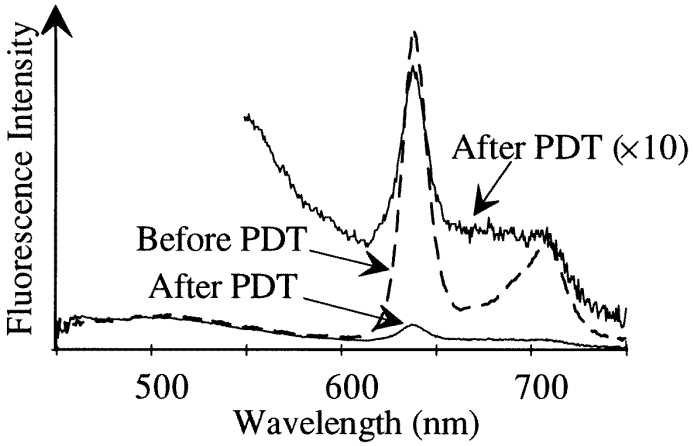

Figure 5. Fluorescence spectra of a nodular basal cell carcinoma on the nose recorded before and after photodynamic treatment using 60 J/cm^2 of red light at 635 nm. The porphyrin peaks are bleached after light delivery and a shoulder is developed at 670 nm.

clearly marked. This instrument thus has the potential to measure the treatment dose delivered to the tissue, as a real-time dosimeter.

The system is a potential candidate as a tool in two main application areas:

• It might prove to offer unique information for the early detection of malignant tumours otherwise not easily observable or to delineate the tumour extent into surrounding tissue. This is mainly of interest for tumours in the bronchial tree, the gastro-intestinal tract, the urinary bladder, the ear, nose and throat region and in the brain. Since the present system is not yet equipped with an endoscopical adapter, the examples here are limited to malignant skin lesions. However, we have obtained images with good demarcation using this system on excised tissue from some organs in low-dose Photofrin injected patients. For most diagnostic applications, one would like to have a false-colour coded contrast function image as an overlay on a normal reflected light image on a TV monitor. For such applications short integration times and fast image processing are required. That could be achieved by using a more powerful light source and specially developed computer software. An endoscopically adapted system with these features is now under development in our laboratory and preliminary studies with that system indicate that this technique can be used to identify malignant lesions in the above mentioned tracts not found with a visual examination (Svanberg *et al* 1995).

• The system might also be useful during photodynamic therapy to monitor the treatment dose delivered. The drug is known to bleach and thereby alter its fluorescence emission spectrum during the treatment. The degree of bleaching is related to the light dose absorbed by the photosensitiser. By monitoring the shape of the photosensitiser fluorescence emission spectrum, a direct measure of treatment dose delivered is thus obtained.

Acknowledgments

Assistance of and fruitful discussions with Sune Montán, Ingrid Wang and David L Lexin are gratefully acknowledged, as is the financial support from the Swedish Cancer Society, the Swedish National Board for Industrial and Technical Development and the Knut and Alice Wallenberg Foundation.

References

Andersson P S, Montán S and Svanberg S 1987 Multispectral system for medical fluorescence imaging *IEEE J. Quantum. Electron.* **QE-23** 1798–805

Andersson T, Berg R, Johansson J, Killander D, Svanberg K, Svanberg S and Yang Yuanlong 1992 Photodynamic therapy in interplay with fluorescence diagnostics in the treatment of human superficial malignancies *Proc. SPIE* **1645** 187–99

Andersson-Engels S and Wilson B C 1992 Fluorescence in oncology: fundamental and practical aspects *J. Cell. Pharmacol.* **3** 48–61

Andersson-Engels S, Johansson J and Svanberg S 1994 Medical diagnostic system based on simultaneous multi-spectral fluorescence imaging *Appl. Opt.* **33** 8022–9

Andersson-Engels S, Elner Å, Johansson J, Karlsson S-E, Salford LG, Strömblad L-G, Svanberg K and Svanberg S 1991 Clinical recording of laser-induced fluorescence spectra for evaluation of tumour demarcation feasibility in selected clinical specialities *Lasers Med. Sci.* **6** 415–24

Hirano T, Ishizuka M, Suzuki K, Ishida K, Suzuki S, Miyaki S, Honma A, Suzuki M, Aizawa K, Kato H and Hayata Y 1989 Photodynamic cancer diagnosis and treatment system consisting of pulse lasers and an endoscopic spectro-image analyzer *Lasers Life Sci.* **3** 1–18

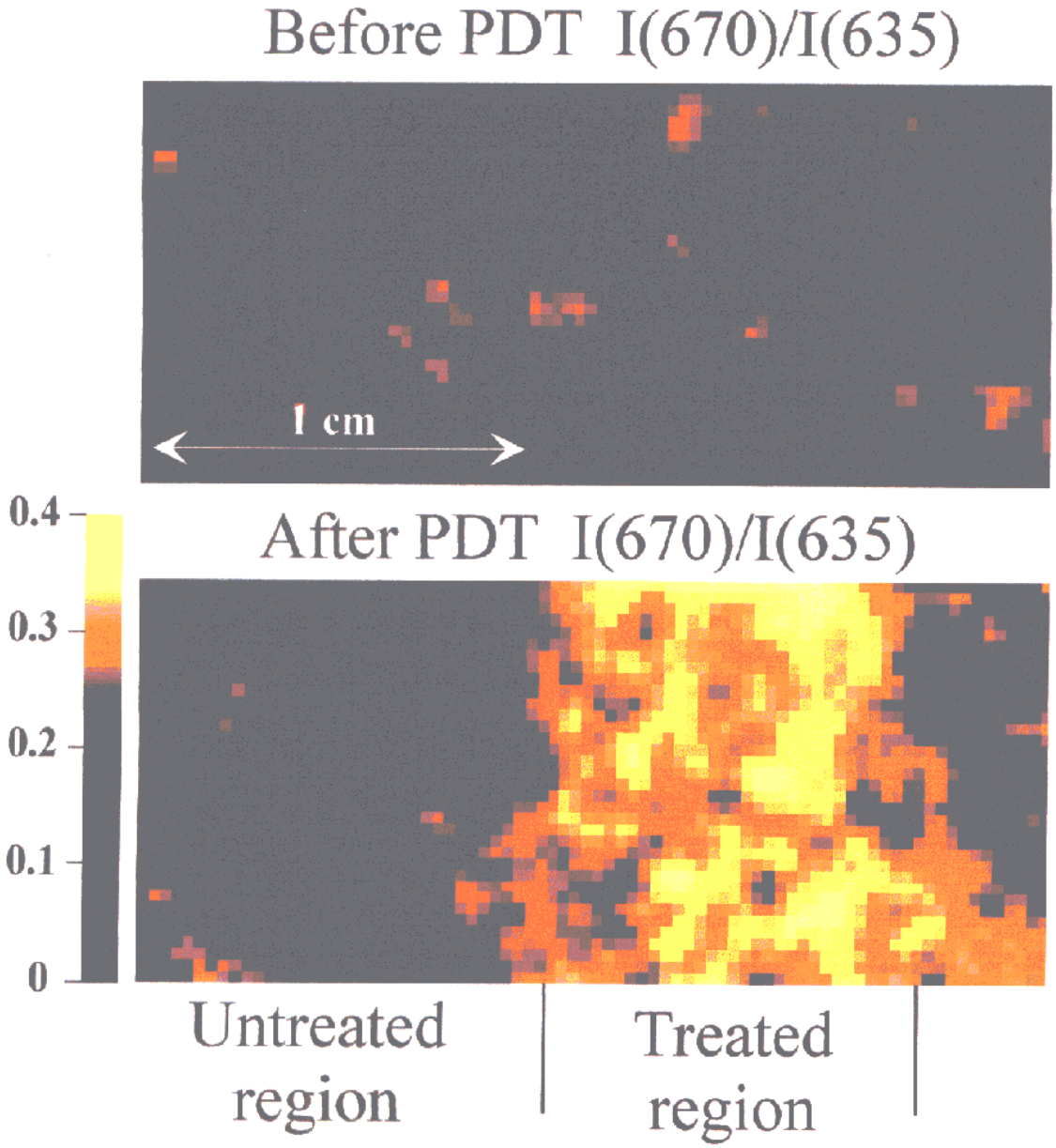

Figure 6. Processed fluorescence images of an ALA sensitised rat liver *in vivo* before and after photodynamic treatment using 15 J/cm^2 of red light at 635 nm. The ratio of the two intensities at 670 nm and 635 nm clearly indicates the treated region.

Kennedy J C and Pottier R H 1992 Endogenous protoporphyrin IX, a clinically useful photosensitiser for photodynamic therapy *J. Photochem. Photobiol. B:Biol.* **14** 275–92

Kennedy J C, Pottier R H and Pross D C 1990 Photodynamic therapy with endogenous protoporphyrin IX: basic principles and present clinical experience *J. Photochem. Photobiol. B:Biol.* **6** 143–8

König K, Wabnitz H and Dietel W 1990 Variation in the fluorescence decay properties of haematoporphyrin derivative during its conversion to photoproducts *J. Photochem. Photobiol. B:Biol.* **8** 103–11

Lam S, MacAuley C, Hung J, Leriche J, Profio A E and Palcic B 1993 Detection of dysplasia and carcinoma in situ with a lung imaging fluorescence endoscopic device *J. Thorac. Cardiovasc. Surg.* **105** 1035–40

Lohmann W, Mussmann J, Lohman C and Künzel W 1989 Native fluorescence of the cervix uteri as a marker for dysplasia and invasive carcinoma *Europ. J. Obstetr. Gynecol. Reprod. Biol.* **31** 249–53

Lohmann W and Paul E 1989 Native fluorescence of unstained cryosections of the skin with melanomas and naevi *Naturwissenshaften* **76** 424–6

Moan J 1988 A change in the quantum yield of photoinactivation of cells observed during photodynamic

treatments *Lasers Med. Sci.* **3** 93–7
Moan J, Rimington C and Malik Z 1988 Photoinduced degradation and modification of Photofrin II in cells *in vitro. Photochem. Photobiol.* **47** 363–7
Palcic B, Lam S, Hung J and MacAuley C 1991 Detection and localization of early lung cancer by imaging techniques *Chest* **4** 742–3
Profio A E 1990 Fluorescence diagnosis and dosimetry using porphyrins *Photodynamic Therapy of Neoplastic Disease.* vol. I, ed D Kessel (Boca Raton, Fl: CRC Press) pp 77–89
Schneckenburger H, Lang M, Köllner T, Rück A, Herzog M, Hörauf H and Steiner R 1989 Fluorescence spectra and microscopic imaging of porphyrins in single cells and tissues *Lasers Med. Sci.* **4** 159–66
Svanberg K, Andersson T, Killander D, Wang I, Stenram U, Andersson-Engels S, Berg R, Johansson J and Svanberg S 1994 Photodynamic therapy of non-melanoma cancers of the skin utilizing topical δ-amino levulinic acid application and laser irradiation *Br. J. Dermatology* **130** 743–51
Svanberg K, Wang I, Colleen S, Idvall I, Ingvar C, Lundgren R, Rydell R, Jocham D, Knipper A, Thomas S, Diddens H, Bown S, Grant G, Montán S, Jonsson I, Andersson-Engels S and Svanberg S 1995 Clinical multi-colour fluorescence imaging of malignant tumours - initial experience, to appear
Unsöld E, Baumgartner R, Beyer W, Jocham D and Stepp H 1990 Fluorescence detection and photodynamic treatment of photosensitised tumours in special consideration of urology *Lasers Med Sci.* **5** 207–12